Chapter 5
Comparative Study of the Dynamic Fracture Toughness Determination of Brittle Materials Using the Kolsky-Hopkinson Bar Machine

Pengwan Chen, Baoqiao Guo and Jingjing Chen

5.1 Introduction

Due to its high strength and hardness, high temperature resistance and low cost, alumina ceramics are widely used in a large range of applications such as armor systems, aerospace industry. In these cases, the ceramic materials inevitably subjected to dynamic loading, its dynamic mechanical properties consequently become the criterion. Fracture toughness is the key parameter in fracture mechanics, which defines a material's resistance to crack propagation for plain strain loading. Measuring this parameter requires knowledge of the specimen geometry and a preset crack within the material. Metals are ductile materials and have traditionally used pre-notch methods to grow a natural crack starter. However, it's difficult to machine a three-point bending (TPB) specimen for brittle materials because of low tensile strength.

The ceramics are typical brittle materials, of which the tensile strength is much lower than the compressive strength. Furthermore, the dynamic fracture toughness is loading rate related. It's even hard to measure the dynamic fracture toughness of ceramic materials. Because of the simplicity of the sample preparation and the experiment process, the Brazilian test has become a standard method and widely used in measuring the dynamic tensile strength of brittle materials such as rock, concrete and ceramic [1–3]. As the most common dynamic impact loading device, the split Hopkinson pressure bar (SHPB) technique [4] is widely used in mechanical study of brittle material [5–8].

P. Chen (✉) · B. Guo · J. Chen
State Key Laboratory of Explosion Science and Technology,
Beijing Institute of Technology, Beijing 100081, China
e-mail: pwchen@bit.edu.cn

R. Othman (ed.), *The Kolsky-Hopkinson Bar Machine*,
https://doi.org/10.1007/978-3-319-71919-1_5

Based on the standard Brazilian test, Wang et al. [9, 10] proposed the flatted Brazilian disc (FBD) test, by which the indirect tensile strength and the fracture toughness of brittle materials could be determined. Chong and Kuruppu also proposed the notched semi-circular bending (NSCB) test to measure the fracture toughness of brittle materials [11].

For the rocks, the dynamic fracture phenomena are frequently encountered in geophysical processes and engineering applications such as the earthquake, projectile penetration, rock blasts [12, 13]. As typical brittle materials, rocks are the mostly studied materials in both static and dynamic tests. Many testing standards on brittle materials mainly come of rocks [14–17].

The dynamic fracture toughness plays an important role in mechanical properties of alumina ceramics. Samborski presented the experimental results of static and dynamic fracture toughness of alumina, and analyzed the influence of porosity fraction on fracture toughness [18]. However, the loading rate effect on the fracture toughness was not investigated. Wang et al. [19] measured dynamic tensile strength of a brittle rock using FBD test, but the time to equilibrium and pattern of stress distribution for different FBD sample was given by finite element analysis. Xia et al. studied the loading rate dependence of fracture toughness on rock [20] and PMMA [21]. PMMA is typical polymer and it shows a non-linear ductile behavior in static case [22]. Due to the strain-rate effect, PMMA presents the brittle behavior from the dynamic deformation and failure in dynamic Brazilian tests [23]. Rittel and Maigre studied the dynamic fracture of PMMA using the so-called compact compression specimen (CCS) configuration [24], the results of dynamic fracture toughness present loading related dependency.

Recently, the digital image correlation (DIC) method has become widely applied in experimental mechanics as a practical and effective tool for full-field deformation measurement [25, 26]. Zhang and Zhao studied the loading rate related dynamic toughness of rocks by NSCB test [27]. The dynamic deformation and failure was also analyzed by the strains fields measured DIC. In the same way, Chen et al. measured the dynamic fracture toughness and failure behavior of explosive mock materials [28]. In the review researches on the dynamic tests on rocks [12, 13], the comprehensive details have been presented on the development of split Hopkinson bar techniques, high rate deformation measurement techniques, the samples geometrical configurations, and etc.

A comparative study using the TPB, NSCB and FBD tests was presented to determine the fracture toughness of a polymer-bonded explosive simulant [29]. The results of three different tests were in good agreement. But the tests were performed only in static, the stain rate effects were not performed.

In this study, the dynamic deformation and failure process, the dynamic fracture toughness on the alumina ceramic and PMMA was experimentally studied by using a SHPB apparatus and high speed DIC technique. The loading rate related dynamic fracture toughness was measured by using three test methods: FBD test, NSCB test and TPB test. The results were analyzed and the testing methods for testing dynamic properties of brittle materials was discussed.

5.2 Testing Principle and Experimental Setup

By using a SHPB apparatus, the dynamic tests were performed on two different materials: alumina ceramic and PMMA. The dynamic fracture toughness at different loading rates was measured by three test methods: the FBD test, the NSCB test and the TPB test. The FBD and NSCB samples are machined from the standard Brazilian disc. The disc dimensions made of alumina ceramic are Φ40 × 18 mm, and those of PMMA are Φ32 × 13 mm. The mechanical principles and the theoretical equations of these three testing methods are therefore introduced.

5.2.1 Flatted Brazilian Disc (FBD) Test

In standard Brazilian disc test, the stress concentration on the loading points may cause the pre-crack. As an alternative, Wang et al. [9, 10] proposed the FBD test. As shown in Fig. 5.1, two parallel planes are processed as the top and bottom surfaces of the disc sample. The pair of loads are applied on the two flat planes. According to Griffith's strength theory, the crack initiates in the center of the FBD sample in condition that the loading angle $2\alpha \geq 20^{\circ}$, which is the critical prerequisite for the validation of the tensile strength and the fracture toughness. The tensile strength and fracture toughness can also be achieved by this proposed test. The tensile strength of FBD sample is expressed as:

$$\sigma_t = k\frac{2P_t}{\pi DB} \tag{5.1}$$

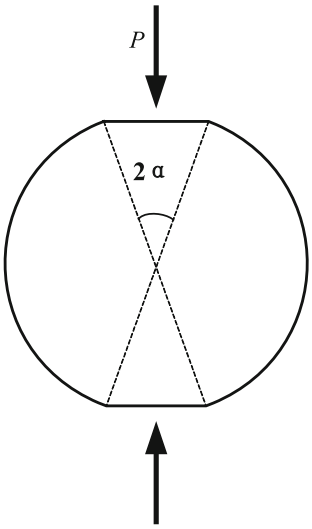

Fig. 5.1 Schematic of FBD test

where P_t is the maxi load, D and B are the disc diameter and thickness respectively. The coefficient k, which mainly related to the loading angle α, can be determined by finite element analysis and in the case of standard Brazilian, the loading angle $2\alpha = 0°$, we get $k = 1$.

At the same time, the fracture toughness of FBD sample can be obtained by

$$K_{IC} = \frac{P_{cr}}{B\sqrt{D/2}}\Phi \tag{5.2}$$

where P_{cr} is on the local inflection point after the failure load P_t, which will be demonstrated in the subsequent experimental tests. Φ is a coefficients relevant to load angle. From the finite element analysis on the FBD sample by Wang et al. [10], the crack initiates in the sample center when the flat angle is under the condition $20° \leq 2\alpha \leq 30°$. Two coefficients k and Φ can also be achieved by from the numerical analysis. In this study, the loading angle is $2\alpha = 30°$, so we get $k = 0.9205, \Phi = 0.5895$.

5.2.2 Notched Semi-circular Brazilian (NSCB) Test

Proposed by Chong and Kuruppu [11], the fracture toughness of brittle materials such as rock was studied by the NSCB test. Compared to the TPB test, the NSCB sample is compact. That's great advantage for sample preparation and also the dynamic test with SHPB device. As shown in Fig. 5.2, the NSCB sample with a pre-fabricated crack is supported by two brackets, and the load is applied in the middle of sample. The fracture toughness of NSCB can be determined by

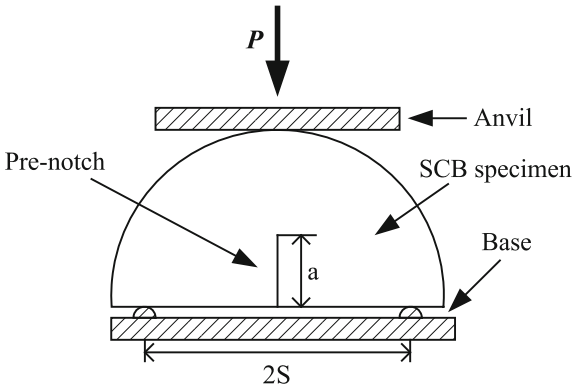

Fig. 5.2 Schematic of NSCB test

$$K_{IC} = \frac{P_Q\sqrt{\pi a}}{DB} Y_K(x) \tag{5.3}$$

$$Y_K(x) = 4.47 + 7.4\frac{a}{D} - 106(\frac{a}{D})^2 + 433.3(\frac{a}{D})^3, \quad \text{where} \quad x = \frac{a}{D}, \frac{2S}{D} = 0.8, \tag{5.4}$$

where P_Q is critical damage load, D and B are the diameter and thickness of sample, α is the pre-fabricated crack length, Y_K is a function of a/D and $2S$ (the bending span). Equations 5.3 and 5.4 are valid only when the conditions are satisfied: $0.25 \leq 2\alpha \leq 0.35$ and $2S/D = 0.8$. The pre-fabricated crack length of NSCB samples made of alumina ceramic is $a = 12$ mm. For the NSCB samples of PMMA, $a = 9.6$ mm.

5.2.3 Three-Point Bending (TPB) Test

The three-point bending test is common method to determine the fracture toughness of metal materials, as illustrated in Fig. 5.3. The fracture toughness K_{IC} of the long rectangular sample with a pre-crack can be determined by:

$$K_{IC} = \frac{P_q \cdot S}{B \cdot W^{3/2}} f(x) \tag{5.5}$$

$$f(x) = \frac{3x^{1/2}[1.99 - 2.15x(1-x) - 3.93x + 2.7x^2]}{2(1+x)(1-x)^{3/2}}, \quad x = \frac{a}{W} \tag{5.6}$$

where $B \times W \times S$ are the thickness, height and the length between the two supports, a is the length of pre-crack, and P_Q is the failure load. In the current study, the dimensions of TPB samples both for alumina ceramic and PMMA are $B \times W \times S$ = 5 mm × 10 mm × 30 mm, and the length of pre-crack is $a = 2$ mm.

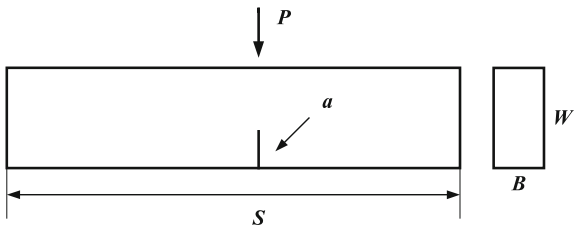

Fig. 5.3 Schematic of TPB test

5.2.4 Sample Preparation and Experimental Setup

The samples made of fine alumina ceramics powder, were prepared by cold compression molding and then sintered under very high temperature. The relative density is about 94.3%. The diameter and thickness of disc-like samples are $\Phi 40 \times 16$ mm. The FBD and NSCB samples were machined from the original disc samples. The diameters of those two samples are the same with the original disc sample. The flat angle of the flat Brazilian disc is 30°.

In this work, a SHPB system was used as the dynamic loading device. The samples were placed between the incident bar and the transmitted bar. The SHPB apparatus dynamic testing system with the geometrical configuration of three different samples is illustrated in Fig. 5.4. The strain signals from the strain gages attached on the incident and transmitted bars, were recorded by the dynamic strain indicator. a high speed (HS) camera (type Photron Fastcam SA5) was used to measure the dynamic displacement and strain fields.

The HS camera and dynamic strain indicator are simultaneously triggered by the shifting signal generated from the velocity meter. The digital images and stress wave signals are then recorded simultaneously by the high speed camera and dynamic strain indicator. The typical incident, reflected and transmitted pulses recorded in the Brazilian test of the alumina ceramic are shown in Fig. 5.5.

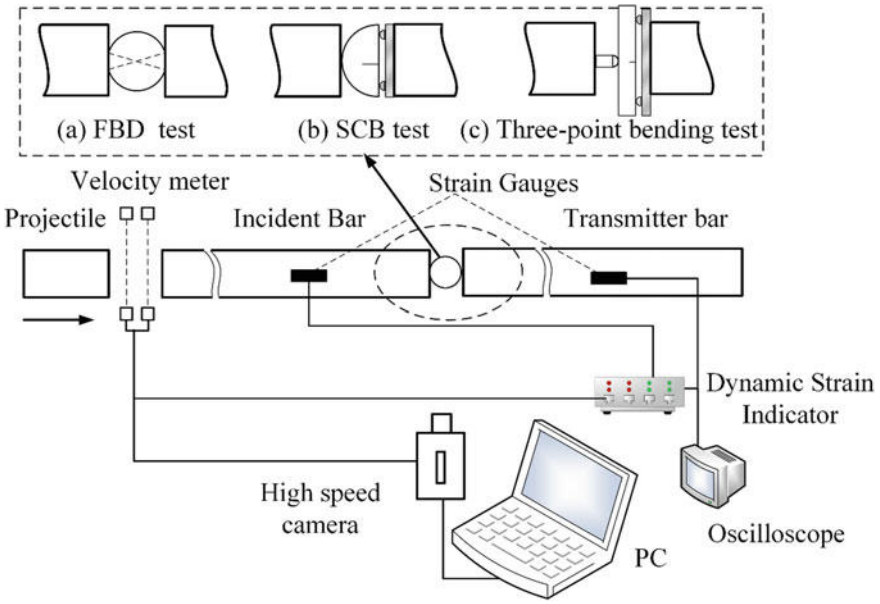

Fig. 5.4 Schematic of the experimental setup

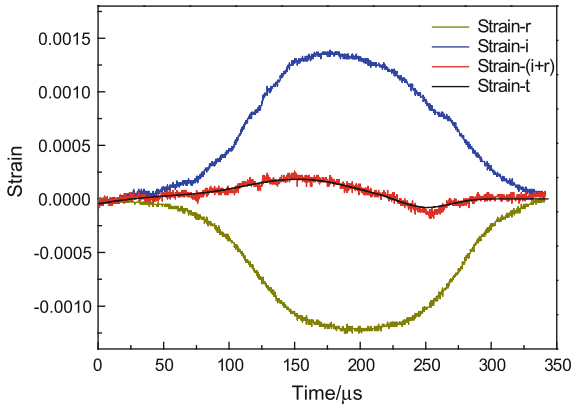

Fig. 5.5 Typical incident, reflected, and transmitted strain pulses of alumina ceramic NSCB sample

5.3 Dynamic Deformation and Failure Analysis

From the pulses measured by the strain gage technique, the stress-strain curve can be deduced. Form the above testing system, the dynamic kinematic fields can be calculated from the images captured by HS camera. This proves a quantitative and evidence information for the analysis on the dynamic deformation and the fracture procedure of the tested materials. In this section, the results only on alumina ceramic will be presented. The deformation and failure mode are found similar on PMMA. The results on PMMA will not be redundantly presented.

The displacement vector fields of NSCB sample at different moments are shown in Fig. 5.6. The frame rate is 75,000 fps, and the image resolution is 320 × 264 pixels. The results show that the local tensile strain concentration appears obviously at pre-fabricated crack tip at 40.0 μs, and the crack propagates till finally the sample is split into two parts, which rotate oppositely around the left point contacted by the incident bar. The Displacement vector fields are illustrated in Fig. 5.7. At 160 μs, it's obvious the two parts are rotating oppositely.

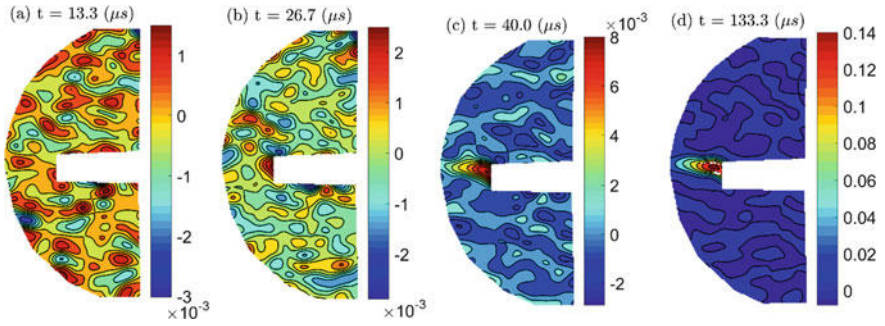

Fig. 5.6 Tensile strain fields of NSCB sample at different moments

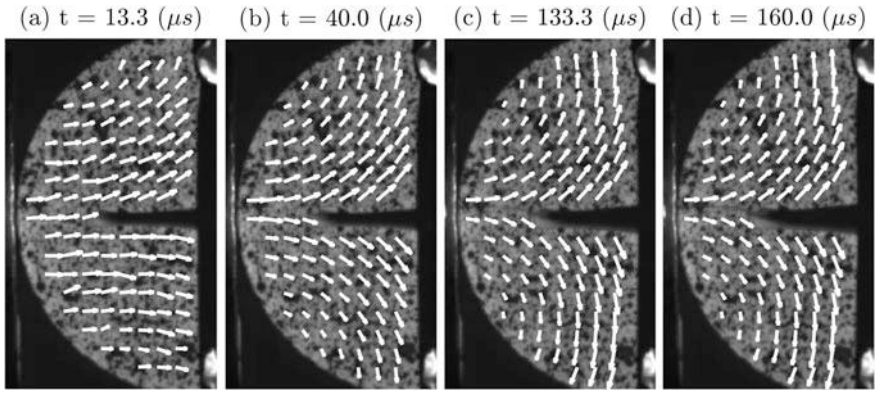

Fig. 5.7 Displacement vector fields of NSCB sample at different moments

From the above NSCB tests, the images on nearly whole surface are recorded and the frame rate is less than 100,000 fps. The deformation fields are calculated by DIC on whole surface of the samples. However, the frame rate is not enough high, only the main crack steps are observed and analyzed. It's difficult to study the crack propagation process of brittle materials from the raw images captured by high-speed camera. In order to observe the details on the crack propagation, the frame rate should be higher, while the image resolution will be decreased. Instead on the whole surface of sample, the deformation fields only on the local area of crack tip are measured. This can improve the displacement resolution. By the combined high-speed DIC-SHPB system, the crack propagation process of alumina ceramic under dynamic loading is therefore studied.

For the NSCB test, the images of resolution 128 × 128 pixels on the local zone of crack tip were taken at frame rate 210,000 fps. The time interval between two images is 4.76 μs. As shown in Fig. 5.8a, three pairs of points on both sides of the crack extension path are chosen, which are indicated by **E1**, **E2** and **E3**. From the displacement fields measured by DIC technique during the dynamic deformation process, the COD (crack opening displacement) curves in function of time of between each pair of points can be extracted. The dynamic loading curve is provided by the SHPB device. The COD curves and loading curve are shown in Fig. 5.8b. The COD curves remain approximately zero before the load reaches its peak. It shows that the crack hasn't extended. The load falls sharply after its peak, and the CODs increase linearly in rapid crack open phase. For the linear increasing part of the COD curves, the slope of **E1** is highest and the slope of **E3** is lowest. It's obvious that the crack extends from the pre-fabricated crack tip to the left side till the contact point with the incident bar. The two split parts rotate oppositely around the contact point by the incident bar. The same results are described in Fig. 5.11. From the delay among the three COD curves in Fig. 5.8b, the crack extension speed can be determined.

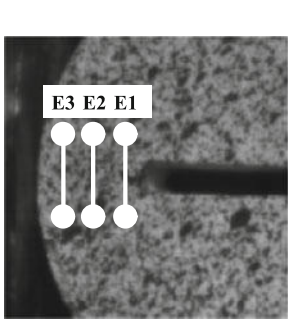

(a) Crack extension in NSCB sample

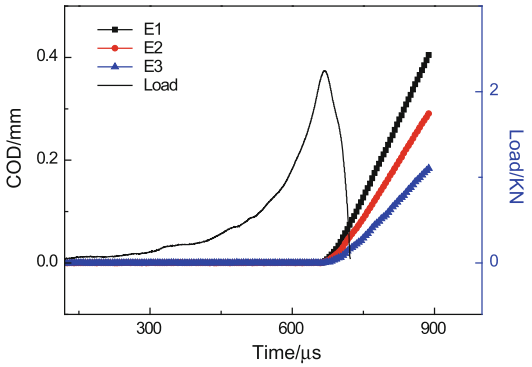

(b) COD curves and loading curve

Fig. 5.8 Crack propagation of NSCB sample under dynamic load, **a** Crack extension in NSCB sample **b** COD curves and loading curve

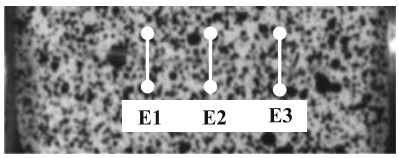

(a) Crack in FBD sample

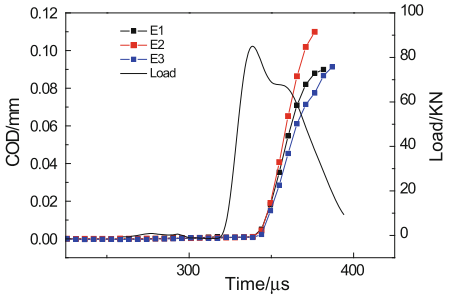

(b) COD curves and loading curve

Fig. 5.9 Crack propagation of FBD sample under dynamic load, **a** crack in FBD sample **b** COD curves and loading curve

In the same way, for alumina ceramic FBD sample, the COD curves on three different locations across the loading diameter are analyzed. As illustrated in Fig. 5.9a, E2 is in the center of the circular sample, E1 and E3 are on its both sides. The frame rate is 100,000 fps. The COD curves as well as the loading curve are shown in Fig. 5.9b. Similar to the NSCB test, the COD curves rise after the maximum loading value, it indicates that the crack begins to extend when the load exceeds the strength of material. The distances of three locations are quite close, there is little different among the COD curves. However, by theoretic analysis, the strain in the center of sample should be maximal. This is confirmed by the COD curves in Fig. 5.9b. The crack initiates in the center (location **E2**) and extends on both sides (location **E1 and E3**) under the dynamic load.

The correlation coefficient presents the matching level between the undeformed and deformed images. The mismatching in local area of the tow images makes the

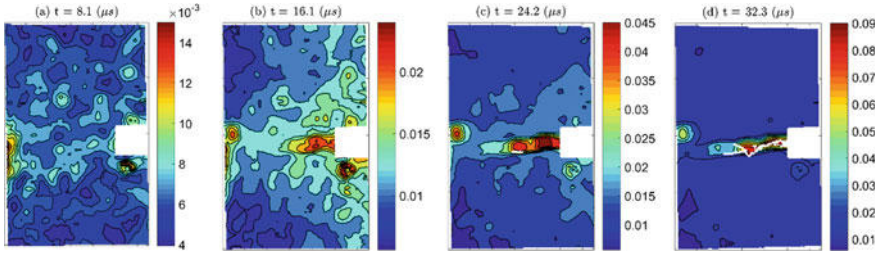

Fig. 5.10 Correlation coefficient fields of NSCB sample at different moments

correlation coefficient map becomes a good indicator of crack and fracture [30]. The correlation coefficient fields of TPB sample at different moments during the dynamic fracture procedure are presented in Fig. 5.10. The image size is 192 × 224 pixels at 124,000 fps. From the contour plots of the correlation coefficient, the crack initiation and propagation can be detected.

5.4 Determination of the Dynamic Fracture Toughness of Brittle Materials

As presented in the precedent section, the FBD test not only can achieve the strength, but also can provide the fracture toughness. Furthermore, the sample is compact and it's not necessary to fabricate the pre-crack. It's a big advantage in sample preparation for brittle material. The curve of stress intensity factor $K_I(t)$ can be obtained according to the Eq. (5.2), as shown in Fig. 5.11. After the collision and compaction process at initial contact, the stress intensity factor $K_I(t)$ curve changes over time with the load increases. There is a linear phase before the peak in the $K_I(t)$ curve, the slope of the linear phase is the dynamic loading rate $\mathrm{d}K_I/\mathrm{d}t$. Because the section of circular samples along the loading direction is not constant, the loading rate instead of the strain rate is presented in this study. The damage occurs when the load reaches the maximum; the cracks appeared in the center of the disc, and growth with the loading increase. And the crack went throughout the disc only when the load down decreased to local inflection load. Therefore, P_{cr} at inflection point represents the load of fracture toughness.

Based on the previous analysis, the crack initiate at the maximum load, and crack penetrate at the local minimum load P_{cr}. The time interval between the maximum load and P_{cr} (Δt in Fig. 5.11) can be determined. As the radius of the disc is known, the crack propagation velocity of alumina ceramic can be determined in the FBD test. The velocity is determined about 2300 ± 200 m/s.

For the NSCB test with the pre-fabricated crack, the fracture toughness of alumina ceramics can be calculated with relevant parameters according to Eqs. (5.3) and (5.4). The dynamic loading rate calculation method of NSCB test is the same

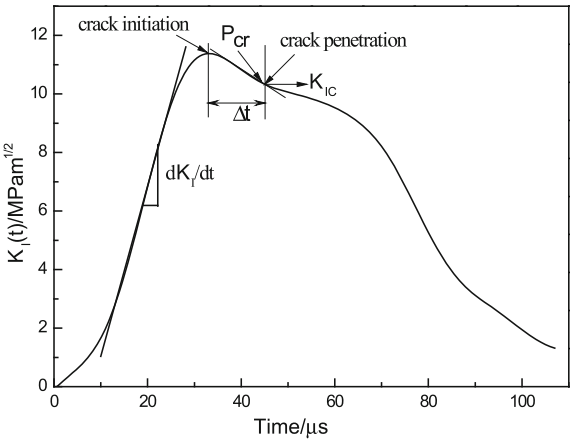

Fig. 5.11 Typical stress intensity factor curve of FBD test

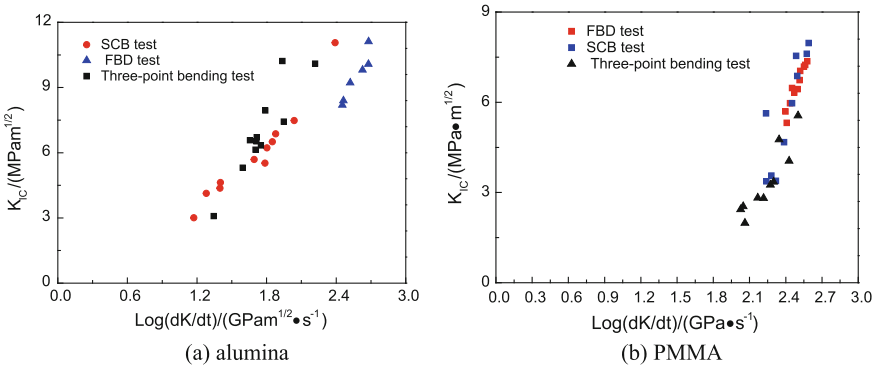

Fig. 5.12 Dynamic fracture toughness in function of strain rate by three test methods

with the FBD test. The relationship between fracture toughness of alumina ceramics with two densities measured by TPB test, FBD test and NSCB test and loading rate is shown in Fig. 5.12a. The fracture toughness measured by three methods are increased with the loading rate, and the three methods have good consistency. The loading rate dependence of alumina ceramics fracture toughness is presented by Kishi [31], it is consistent with the result of in this work. The results of dynamic fracture toughness of PMMA measured by three test methods are presented in Fig. 5.12b. The results are the obvious loading rate related, which is similar as the alumina ceramic. The effectiveness of FBD test to measure fracture toughness of the brittle material was verified by comparing those three methods. The FBD test has certain advantages in the aspect of toughness measurement for brittle material fracture because of sample preparation is simple and it does not need to prefabricate crack in the sample.

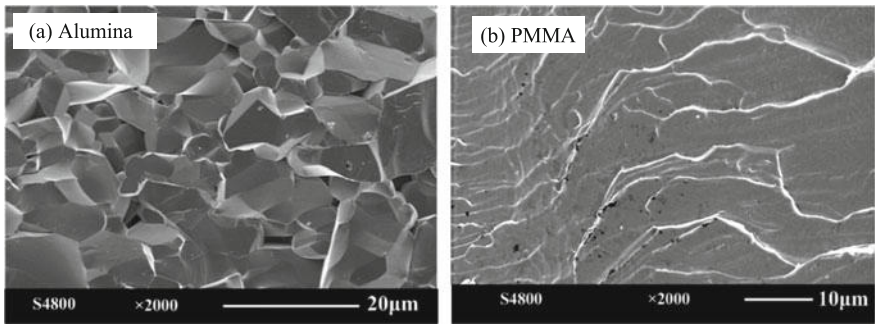

Fig. 5.13 Micro morphologic observation of three tested brittle materials on the fracture section by SEM

5.5 Micro Morphologic Analysis on the Fracture

The microstructures of the two tested brittle materials are very different. In dynamic Brazilian test, the disc samples are split into two parts along the loading direction. Figure 5.13 illustrates the micro morphologic observation of three tested brittle materials on the fracture section by SEM. It can be observed that the two materials appear the brittle fracture characteristic. The broken section of alumina ceramic appears the sugar candy-like fracture (Fig. 5.13a), and the cracks propagate along the interfaces of little particles. It's typical transgranular fracture. PMMA is high molecular polymer, and its broken section appears river-like brittle fracture (Fig. 5.13b).

5.6 Discussion and Conclusion

In this study, we made a comparative study of the dynamic fracture toughness of alumina ceramic by three test methods: FBD test, NSCB test and TPB test. The dynamic fracture toughness of alumina ceramic and PMMA exhibits an obvious rate dependence upon the loading rate. The result shows the reliability of the three methods to determine the dynamic fracture toughness of brittle materials. However, the FBD samples are not necessary to fabricate a pre-crack. In addition, the FBD test can also measure the dynamic tensile strength. Considering these advantage, the FBD test is recommended as an alternative method for measuring the dynamic fracture toughness of brittle materials.

References

1. Johnstone C, Ruiz C (1995) Dynamic testing of ceramics under tensile stress. Int J Solids Struct 32(17/18):2647–2656
2. Zhao J, Li HB (2000) Experimental determination of dynamic tensile properties of a granite. Int J Rock Mech Min Sci 37(5):861–866

3. Rafael J, Proveti C, Michot G (2006) The Brazilian test: a tool for measuring the toughness of a material and its brittle to ductile transition. Int J Fract 139:455–460
4. Chen WW, Song B (2011) Split Hopkinson (Kolsky) bar design, testing and applications. Springer, USA
5. Zhu J, Shisheng H, Wang L (2009) An analysis of stress uniformity for concrete—like specimens during SHPB tests. Int J Impact Eng 36:61–72
6. Wang S, Liu KX (2011) Experimental research on dynamic mechanical properties of PZT ceramic under hydrostatic pressure. Mater Sci Eng, A 528:6463–6468
7. Chang H, Binner J, Higginson R, Myers P, Webb P, King G (2011) High strain rate characteristics of 3-3 metal-ceramic interpenetrating composites. Mater Sci Eng, A 528:2239–2245
8. Dong S, Xia K, Huang S, Yin T (2011) Rate dependence of the tensile and flexural strengths of glass-ceramic Macor. J Mater Sci 46:394–399
9. Wang QZ, Xing L (1999) Determination of fracture toughness KIC by using the flattened Brazilian disk specimen for rocks. Eng Fract Mech 64:193–201
10. Wang QZ, Jia XM, Kou SQ et al (2004) The flattened Brazilian disc specimen used for testing elastic modulus, tensile strength and fracture toughness of brittle rocks: analytical and numerical results. Int J Rock Mech Min Sci 41:245–253
11. Chong KP, Kuruppu MD (1984) New specimen for fracture toughness determination for rock and other materials. Int J Fract 26:59–62
12. Xia K, Yao W (2015) Dynamic rock tests using split Hopkinson (Kolsky) bar system—a review. J Rock Mech Geotech Eng 7:27–59
13. Zhang QB, Zhao J (2014) A review of dynamic experimental techniques and mechanical behaviour of rock materials. Rock Mech Rock Eng 47(4):1411–1478
14. ASTM (2004) C496/C496 M-04, standard test method for splitting tensile strength of cylindrical concrete samples. ASTM International, West Conshohocken, USA
15. ASTM (2008) D 3967-08: standard test method for splitting tensile strength of intact rock core specimens. ASTM International, West Conshohocken, USA
16. ISRM Testing Commission (1988) Suggested methods for determining the fracture toughness of rock. Int J Rock Mech Min Sci Geomech Abstr 25(2):71–96
17. ISRM Testing Commission (1995) Suggested method for determining mode I fracture toughness using cracked chevron notched Brazilian disc (CCNBD) specimens. Int J Rock Mech Min Sci Geomech Abstr 32(1):57–64
18. Samborski S, Sadowskiw T (2010) Dynamic fracture toughness of porous ceramics. J Am Ceram Soc 93(11):3607–3609
19. Wang QZ, Li W, Xie HP (2009) Dynamic split tensile test of flattened Brazilian disc of rock with SHPB setup. Mech Mater 41:252–260
20. Dai F, Xia K, Zheng H, Wang YX (2011) Determination of dynamic rock mode-I fracture parameters using cracked chevron notched semi-circular bend specimen. Eng Fract Mech 78:2633–2644
21. Huang S, Luo S, Xia K (2009) Dynamic fracture initiation toughness and propagation toughness of PMMA. Proceedings of the SEM Annual Conference June 1–4, 2009
22. Liu C (2010) Elastic constants determination and deformation observation using Brazilian disk geometry. Exp Mech 50:1025–1039
23. Chen J, Guo B, Liu H, Liu H, Chen P (2014) Dynamic Brazilian test of brittle materials using the split Hopkinson pressure bar and digital image correlation. Strain 50(6):563–570
24. Rittel D, Maigre H (1996) An investigation of dynamic crack initiation in PMMA. Mech Mater 23:229–239
25. Pan B, Qian KM, Xie HM, Asundi A (2009) Two-dimensional digital image correlation for in-plane displacement and strain measurement: a review. Meas Sci Technol 20(6):062001–062007
26. Sutton M, Orteu J, Schreier H (2009) Image correlation for shape, motion and deformation measurements: basic concepts, theory and applications. Springer, Berlin

27. Zhang QB, Zhao J (2013) Determination of mechanical properties and full-field strain measurements of rock material under dynamic loads. Int J Rock Mech Min Sci 60:423–439
28. C P, Z Zhongbin, Ma S et al (2011) Measurement of dynamic fracture toughness and failure behavior for explosive mock materials. Front Mech Eng 6(3):292–295
29. Zhou Z, Chen P, Duan Z, Huang F (2011) Comparative study of the fracture toughness determination of a polymer-bonded explosive simulant. Eng Fract Mech 78:2991–2997
30. Zhou Z, Chen P, Huang F, Liu S (2011) Experimental study on the micromechanical behavior of a PBX simulant using SEM and digital image correlation method. Opt Lasers Eng 49:366–370
31. Kishi T (1991) Dynamic fracture toughness in ceramics and ceramics matrix composites. Eng Fract Mech 40(415):785–790